

# Solid State Inclusion of the Nonionic Surfactant C<sub>12</sub>E<sub>4</sub> in $\beta$ -Cyclodextrin, at Various Humidities: A Combined Raman and <sup>13</sup>C CP MAS NMR Study

Luís Cunha-Silva and José J. C. Teixeira-Dias\*

Department of Chemistry, University of Aveiro, P3810-193 Aveiro, Portugal

Received: October 22, 2001

The inclusion of the nonionic surfactant  $\alpha$ -*n*-dodecyl- $\omega$ -hydroxytetra(oxyethylene), C<sub>12</sub>E<sub>4</sub>, in  $\beta$ -cyclodextrin ( $\beta$ CD), has been prepared in the solid state and its structure characterized by powder X-ray diffraction, thermogravimetry, and Raman and <sup>13</sup>C CP/MAS NMR spectroscopies. Stepwise dehydration was observed in the thermogram, indicating the presence of energetically distinct water molecules. Comparison of the dispersions of <sup>13</sup>C chemical shift values for C1 and C4 atoms of the  $\beta$ CD macrocycle, within a series of inclusion compounds of C<sub>*n*</sub>E<sub>*m*</sub> homologues, reveals a rather complete symmetrization of the  $\beta$ CD macrocycle, and the dispersions of <sup>13</sup>C shifts for C6 atoms point to the particular sensitivity of these atoms to hydrogen-bonding type of interactions. The integrated intensity of the O–H Raman stretching band for the  $\beta$ CD inclusion compound of C<sub>12</sub>E<sub>4</sub> is approximately constant for humidities between 20% and 80%. In passing from 15% to 20% of humidity, one observes abrupt relative intensity variations of some Raman bands, in particular at 926 cm<sup>-1</sup>, and the sudden decrease of the dispersions of <sup>13</sup>C chemical shift values for all carbon atoms of the  $\beta$ CD macrocycle. Overall, the above findings converge to stress the structural relevance of hydration water in the  $\beta$ CD inclusion compound of C<sub>12</sub>E<sub>4</sub>.

## 1. Introduction

Crystalline hydrates of  $\beta$ -cyclodextrin (cyclomaltoheptaose,  $\beta$ CD) are good models for the study of hydration processes in biomolecular systems and exhibit interesting properties that have been the subject of a number of studies.<sup>1–6</sup> First of all, the overall crystal structure is known to be preserved for humidities greater than 15%, though with a 2.3% reduction of the cell volume with respect to the 100% humidity level.<sup>1</sup> At low humidities, a distinct phase II with unknown structure is formed.<sup>3</sup> In the range of humidities from 15% to 100%, the water content of crystalline  $\beta$ CD hydrate is in fast equilibrium with atmospheric humidities and, despite the fact that the crystal lattice does not have permanent channels, fast diffusion of water molecules is known to occur due to transient fluctuations in the lattice.<sup>1</sup> Exchange experiments carried out with water marked either with D or <sup>18</sup>O showed that the H/D exchange is complete, hence extending also to sterically unaccessible O–H groups, and that the long-range transport of hydrogen takes place by diffusion of intact water molecules, as indicated by <sup>18</sup>O/<sup>16</sup>O exchange.<sup>2</sup>

$\beta$ CD hydrates have also been investigated by <sup>13</sup>C CP/MAS NMR as a part of a study for discovering the relationship between glycosidic linkage conformation and solid state <sup>13</sup>C chemical shifts, since it has been shown that the resolved C1 and C4 NMR resonances come from each of the seven  $\alpha$ (1 $\rightarrow$ 4)-linked glucopyranose residues present in the macrocycle.<sup>7</sup> In fact, rapid averaging of  $\beta$ CD conformations in solution leads to a single resonance for each set of chemically equivalent carbon atoms.<sup>7</sup> The wide range of chemical shifts observed for C1 and C4 sites was found to be primarily determined by glycosidic linkages conformations, and correlations were found between C1 chemical shifts and the moduli of torsion angles

describing rotation about the C1–O1 and O1–C4' bonds.<sup>7</sup> In turn, the chemical shifts for C6 resonances were found to be sensitive to hydrogen-bonding interactions.<sup>8</sup> On the whole, the carbon atoms of the  $\beta$ CD macrocycle are interesting NMR probes for studying possible conformational changes during hydration or dehydration processes.

Despite its interesting properties as a crystalline hydrate,  $\beta$ CD is better known for its ability to form inclusion complexes, by accommodating guest molecules of suitable size in its cavity.<sup>9</sup> It has been previously suggested that the guest molecules undergo rotational motion inside the cyclodextrin cavity, the motion of smaller guests being least affected by the cavity size of the cyclodextrin.<sup>10</sup> However, hydration characteristics of  $\beta$ CD inclusion compounds have not so far deserved much attention, perhaps because it is generally accepted that, by contrast with  $\alpha$ -cyclodextrin,  $\beta$ CD macrocyclic conformations are similar in the presence or absence of complexing agents.<sup>4</sup> In addition, for the guests generally considered, the encapsulated molecular fragments have little or null conformational flexibility, since they are mostly phenyl groups.

In this work, particular attention as a guest for inclusion in  $\beta$ CD is devoted to  $\alpha$ -*n*-dodecyl- $\omega$ -hydroxytetra(oxyethylene), hereafter referred to as C<sub>12</sub>E<sub>4</sub>, a molecule which belongs to a family of nonionic surfactants of general formula C<sub>*n*</sub>E<sub>*m*</sub> [C<sub>*n*</sub> and E<sub>*m*</sub> stand for CH<sub>3</sub>(CH<sub>2</sub>)<sub>*n*-1</sub>– and –(OCH<sub>2</sub>CH<sub>2</sub>)<sub>*m*</sub>OH moieties, respectively].<sup>11</sup> When the guest displays hydrophobic–hydrophilic behavior, as is the case for C<sub>12</sub>E<sub>4</sub>, the  $\beta$ CD cavity has a tendency to host the hydrophobic fragment or part of it, leaving the hydrophilic moiety to interact mainly with hydroxyl groups of the  $\beta$ CD rims and with hydration water. Considering the diameter of the  $\beta$ CD cavity and the flexibility of the alkylic fragment of C<sub>12</sub>E<sub>4</sub>, the hydrocarbon chain will probably coil inside the cavity, thus effectively increasing the number and strength of  $\beta$ CD-alkylic fragment interactions.<sup>12</sup> In what concerns  $\beta$ CD, it has been previously shown by Raman optical

\* Corresponding author. E-mail: tdias@dq.ua.pt FAX: 351-234370084.

activity that a tighter guest binding leads to an additional reduction in conformational flexibility of the cyclodextrin macrocycle.<sup>13</sup> When obtained from aqueous solution crystallization, the resulting hydrate crystals contain water molecules that may be located in interstitial spaces and, eventually, in  $\beta$ CD cavities.<sup>1</sup> While it is generally accepted that hydration water is known to have an important role in promoting the stability of the inclusion compound, no systematic study of the hydration features of inclusion compounds such as  $C_nE_m$  has been done, to our knowledge.

In this work, a combined Raman and  $^{13}\text{C}$  CP/MAS NMR study is performed for the solid-state inclusion of  $C_{12}E_4$  in  $\beta$ CD at different relative humidities. Although conformational features seem to be the main origin of C1 chemical shifts, the lack of correlation so far found between C4 chemical shifts and conformational effects may point to the existence of other operating effects, namely those which may be caused by the encapsulated guest and/or by different hydration levels. To discern those effects whose origin may be in the guest molecule, special attention will also be paid to those trends that might emerge by comparison of the inclusions in  $\beta$ CD of  $C_nE_m$  guests with different hydrophile/hydrophobe chain lengths, namely,  $C_4E_1$ ,  $C_4E_2$ ,  $C_6E_2$ , and  $C_{12}E_4$ . In addition, the inclusion compound of  $C_{12}E_4$  in  $\beta$ CD is studied at defined relative humidities.

## 2. Materials and Methods

$\beta$ CD, kindly donated by Wacker-Chemie, was recrystallized by slow cooling of concentrated aqueous solutions from 80 °C to room temperature. Crystals were taken from the solvent and exposed to an atmosphere of moderate temperature and humidity (18–23 °C and 50–60% relative humidity). After equilibration with the atmosphere, crystals were ground, not sieved, to obtain a microcrystalline powder.  $\alpha$ -*n*-Alkyl- $\omega$ -hydroxyoligo(oxyethylene)s ( $C_4E_1$ ,  $C_4E_2$ ,  $C_6E_2$ ,  $C_{12}E_4$ ) were obtained from Aldrich and used as received.

To prepare each inclusion compound, a saturated aqueous solution of  $\beta$ CD at 70 °C was heated to 80 °C so that the deposited  $\beta$ CD solid was completely solubilized. An equimolar aqueous solution of  $C_nE_m$  at 80 °C was then added. The resulting solution was continuously stirred for 24 h, at 80 °C. The reaction mixture was then slowly cooled down to room temperature. The white precipitate was then filtered, washed several times with cold water, and exposed to an atmosphere of moderate temperature and humidity (18–23 °C and 50–60% relative humidity). For simplicity, we will hereafter refer to the inclusion compound of  $C_nE_m$  in  $\beta$ CD by the shorthand notation  $\{C_nE_m\}$ . This nomenclature intentionally omits any reference-to-stoichiometric ratios, since these were not determined in this paper for the solid-state inclusions.

Defined relative humidities (RHs) were set up by silica gel for RH = 0%, by various saturated salt solutions (RH = 15%,  $\text{LiCl}\cdot\text{H}_2\text{O}$ ; RH = 20%,  $\text{KCH}_3\text{COO}$ ; RH = 42%,  $\text{Zn}(\text{NO}_3)_2\cdot 6\text{H}_2\text{O}$ ; RH = 58%,  $\text{NaBr}\cdot 2\text{H}_2\text{O}$ ; RH = 78%,  $\text{Na}_2\text{S}_2\text{O}_3\cdot 5\text{H}_2\text{O}$ ; RH = 80%,  $\text{NH}_4\text{Cl}$ ; RH = 93%,  $\text{NH}_4\text{H}_2\text{PO}_4$ ),<sup>14</sup> and by pure water for RH = 100%.

Powder XRD data were collected on a Philips X'pert diffractometer using  $\text{Cu K}\alpha$  radiation filtered by Ni ( $\lambda = 1.5418$  Å). TGA studies were performed on a Mettler TA3000 system, using a heating rate of 1 °C  $\text{min}^{-1}$ , under nitrogen atmosphere, with a flow rate of 30 mL  $\text{min}^{-1}$ . The sample holder was a 5 mm i.d. platinum plate and the sample mass was about 5–10 mg. Raman spectra were obtained on a Bruker RFS 100/S spectrometer, using a Nd:YAG laser line at 1064  $\mu\text{m}$ , with 200

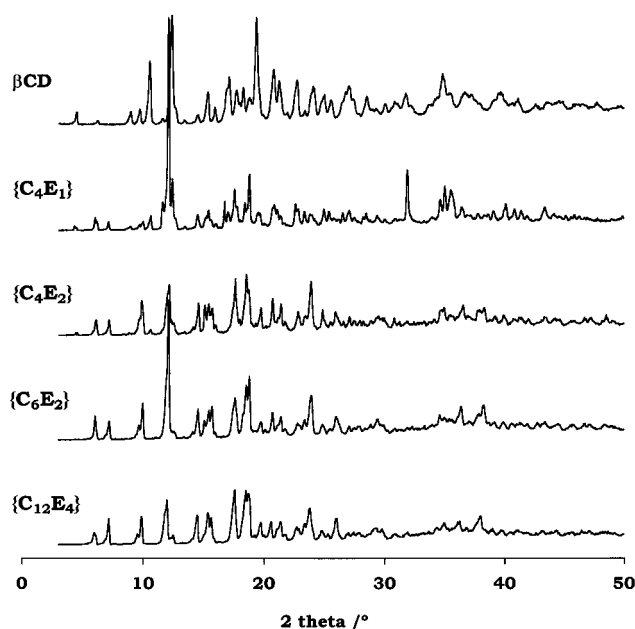


**Figure 1.** Powder X-ray diffraction patterns for  $\beta$ CD,  $\{C_4E_1\}$ ,  $\{C_4E_2\}$ ,  $\{C_6E_2\}$ , and  $\{C_{12}E_4\}$ .

mW of power (resolution 4  $\text{cm}^{-1}$ , 100 scans per spectrum). Solid-state  $^{13}\text{C}$  CP/MAS NMR spectra were recorded at 100.62 MHz, on a 9.4 T Bruker Avance 400 spectrometer (25 °C; 3.6  $\mu\text{s}$   $^1\text{H}$  90° pulses, 2.0 ms contact time, 7–8 kHz spinning rate; 4 s recycle delays). Chemical shifts are quoted in parts per million (ppm) from TMS.

## 3. Results and Discussion

**Powder XRD.** All the above prepared inclusion compounds yielded powder X-ray diffraction patterns (Figure 1), thus indicating that they are crystalline powders. Three distinct groups of diffraction patterns can be easily discerned in Figure 1: group A, which includes the diffraction pattern of  $\beta$ CD; group B, formed by the diffraction pattern for  $\{C_4E_1\}$ ; and group C, which includes the diffraction patterns for  $\{C_4E_2\}$ ,  $\{C_6E_2\}$ , and  $\{C_{12}E_4\}$ . The maxima in the  $\beta$ CD diffraction pattern do not correspond to maxima in the diffraction patterns for group C diffraction patterns, indicating that  $\{C_4E_2\}$ ,  $\{C_6E_2\}$ , and  $\{C_{12}E_4\}$  do not include measurable amounts of  $\beta$ CD, thus being true inclusion compounds.<sup>1</sup> By contrast, medium and intense reflections in the X-ray diffraction pattern for  $\beta$ CD appear as weak or very weak, yet measurable, reflections in the diffraction pattern for  $\{C_4E_1\}$ . In turn, the diffraction patterns for  $\{C_4E_2\}$ ,  $\{C_6E_2\}$ , and  $\{C_{12}E_4\}$  present an appreciable number of coincident reflections among themselves that only become distinct by their intensities.

Considering the sizes of the guest molecules and the relative lengths of their hydrophobic and hydrophilic moieties, the above observations may suggest a cage type of structure for  $\{C_4E_1\}$  similar to the  $\beta$ CD hydrate structure ( $C_4E_1$  is the smaller guest molecule and fits inside the  $\beta$ CD cavity with plenty of free space), and channel structures for the remaining inclusion compounds ( $\{C_4E_2\}$ ,  $\{C_6E_2\}$ , and  $\{C_{12}E_4\}$ ).<sup>9</sup>

**TGA.** Figure 2 presents the thermograms for  $\{C_{12}E_4\}$  and  $\beta$ CD for comparison. By contrast with the thermogram for  $\beta$ CD, where continuous dehydration was observed,<sup>16,17</sup>  $\{C_{12}E_4\}$  undergoes dehydration in a stepwise manner, showing multiple inflection points. The  $\beta$ CD dehydration process ends at approximately 80 °C with a single inflection point around 63 °C and corresponds to an overall mass loss from room temperature

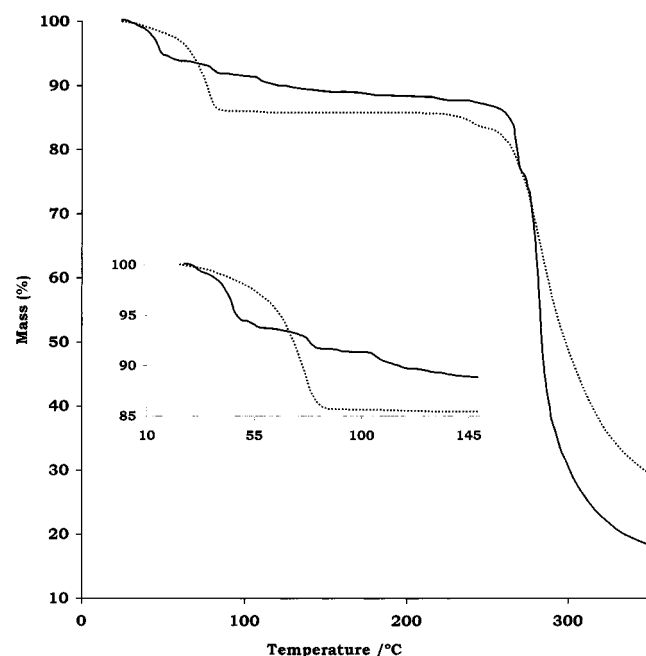


Figure 2. Thermogram for  $\{C_{12}E_4\}$  (continuous line) and  $\beta$ CD (points).

of approximately 14%, that is, 10.3 hydration water molecules per cyclodextrin molecule. In turn, thermal dehydration of  $\{C_{12}E_4\}$  proceeds in multiple dehydration steps and corresponds to a total mass loss of 11% (9.0 water molecules per cyclodextrin molecule, assuming a 2:1 stoichiometry ( $\beta$ CD) $_2$ . $C_{12}E_4$ ), as found for the inclusion complex in aqueous solution<sup>15</sup>.

The multiple dehydration steps are a clear indication of energetically distinct types of hydration water molecules in  $\{C_{12}E_4\}$ , a conclusion whose importance can be stressed by comparing the thermograms for  $\beta$ CD,  $\{C_4E_1\}$ ,  $\{C_4E_2\}$ , and  $\{C_6E_2\}$  (Figure 3). Clearly, there is an increase in the number of inflection points along this series of compounds. While we do not know the host-guest stoichiometries, we can reasonably assume a 1:1 stoichiometry for  $\{C_4E_1\}$  and 2:1 for  $\{C_{12}E_4\}$ .<sup>15</sup> On this basis, the number of water molecules per cyclodextrin is found to be 11.3 for  $\{C_4E_1\}$  (14% mass loss), and 9.0 for  $\{C_{12}E_4\}$  (11% mass loss). In addition,  $\{C_4E_2\}$  has 10.1–10.7 water molecules per  $\beta$ CD (13% mass loss) and  $\{C_6E_2\}$  10.2–11.0 water molecules per  $\beta$ CD (13% mass loss), values which correspond to 2:1 or 1:1 stoichiometries, respectively.

**Raman Spectra.** Considering the inclusion complex stoichiometry and the relative number of vibrational oscillators of each type in  $\beta$ CD and  $C_{12}E_4$ , the Raman spectrum for  $\{C_{12}E_4\}$  is mostly determined by  $\beta$ CD bands. Comparison of the Raman spectrum for  $\{C_{12}E_4\}$  with that for the 2:1  $\beta$ CD: $C_{12}E_4$  physical mixture does not reveal, in general, significant shifts between corresponding Raman bands, and the widths of groups of overlapping bands are similar in both spectra (not shown), thus suggesting that the observed band shapes differences should result mainly from conformational changes during encapsulation. This is not surprising, since the host-guest interactions are noncovalent, and the  $\beta$ CD macrocycle imposes geometrical constraints on the guest, which are likely to restrict the number of conformational states for the encapsulated guest.

The interpretation of the Raman spectra of  $C_nE_m$  has been previously done in terms of conformational states.<sup>18,19</sup> In the solid and in micellar form, three basic conformations have been previously suggested for the interpretation of Raman spectra for this kind of nonionic surfactants: a planar zigzag (symmetric) conformation, a meander (intermediate) conformation,

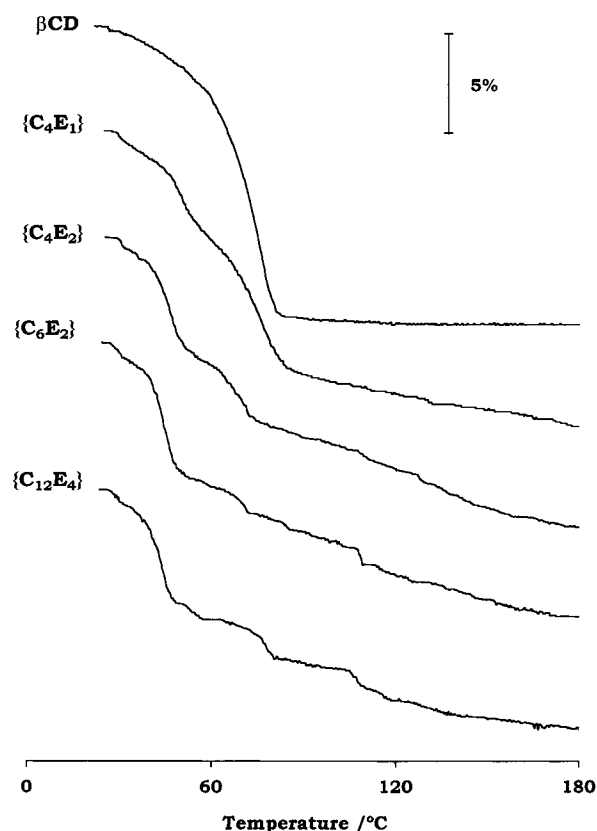
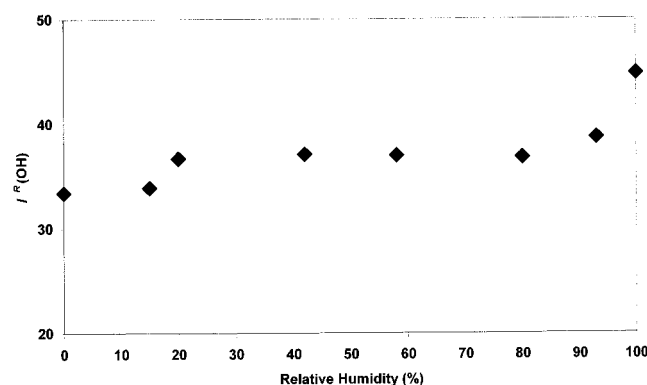


Figure 3. Thermograms for  $\{C_4E_1\}$ ,  $\{C_4E_2\}$ ,  $\{C_6E_2\}$ , and  $\{C_{12}E_4\}$ , from room temperature up to 180 °C.

and a coiled (helical) conformation.<sup>18</sup> For  $C_{12}E_4$ , the latter conformation in which all the dihedral angles are trans, except those about the CC–CO and all the OC–CO dihedral axes, which are gauche, has been previously identified as the single form present in the crystalline phase at liquid nitrogen temperature,<sup>19</sup> thus being considered as a strong candidate for the lowest energy form. When compared with the Raman spectrum for the crystalline solid state at liquid nitrogen temperature, the Raman spectrum for liquid  $C_{12}E_4$  at room temperature presents relatively broad bands, thus pointing to a dispersion of molecular conformations. In turn, comparison of the Raman spectrum for liquid  $C_{12}E_4$  with the  $\{C_{12}E_4\}$ – $\beta$ CD difference spectrum points to a decrease of the zigzag conformation and to an increase of the coiled conformation, in consonance with the results of the model system calculations.<sup>15</sup>

As it has been previously shown, the integrated intensity of the O–H Raman stretching band ( $I_{OH}$ ) of crystalline  $\beta$ CD hydrate exhibits a linear response to variations of ambient humidity for humidities greater than 15%.<sup>20</sup> By contrast,  $I_{OH}$  for  $\{C_{12}E_4\}$  does not present a linear variation over the whole range of relative humidities (Figure 4). Over the whole range of relative humidities,  $I_{OH}$  varies by roughly a fourth of the value at 100% humidity and presents an almost constant  $I_{OH}$  value for humidities between 20% and 80%. In turn, in passing from 20% to 15% of humidity, there is a  $I_{OH}$  decrease of approximately 8%, and between 80% and 100% one observes an 18%  $I_{OH}$  increase.

Figure 5 shows Raman bands for  $\{C_{12}E_4\}$  at defined relative humidities, in the 895–970 and 1280–1365  $cm^{-1}$  regions. The bands at 926, 936, 948, 1329, and 1338  $cm^{-1}$  are ascribed to  $\beta$ CD, whereas the band at 1305  $cm^{-1}$  is mainly due to  $C_{12}E_4$ . In both of these wavenumbers regions, one can discern two groups of relative humidities: one is composed by 0% and 15%



**Figure 4.** Integrated intensity of the O–H Raman stretching band ( $I_{OH}$ ) for  $\{C_{12}E_4\}$  at defined relative humidities.

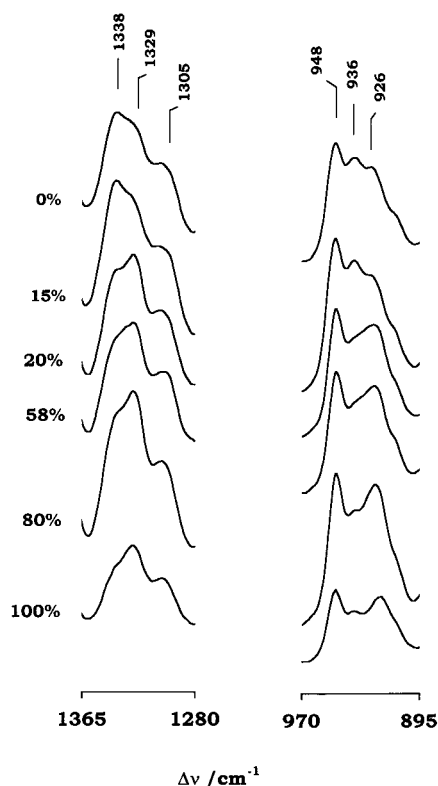


**Figure 5.** Raman bands for  $\{C_{12}E_4\}$  at defined relative humidities, in the 895–970 and 1280–1365  $\text{cm}^{-1}$  regions.

humidities, the other by humidities from 20% up to 100%. In particular, a relative intensification of the 926  $\text{cm}^{-1}$  band is clearly observed in passing from the first group of humidities (0% and 15%) to the second (from 20% up to 100%). Incidentally, this spectral region has been the subject of a previous Raman optical activity study, because a  $\beta$ CD Raman band at around 920  $\text{cm}^{-1}$  was found to be a signature for the dispersion of conformations around the glycosidic linkage in the  $\beta$ CD macrocycle.<sup>13</sup>

**$^{13}\text{C}$  CP/MAS NMR.** In the range of cyclodextrin resonances, the  $^{13}\text{C}$  CP/MAS NMR spectrum for  $\{C_{12}E_4\}$  reveals features that easily stand out of comparison with the spectra for  $\beta$ CD,  $\{C_4E_1\}$ ,  $\{C_4E_2\}$ , and  $\{C_6E_2\}$  (Figure 6). While the centers of the multiple resonances observed for each type of carbon atom do not present significant chemical shift changes, the multiplicity of signals for each carbon atom is progressively reduced along the series of spectra for  $\{C_4E_2\}$ ,  $\{C_6E_2\}$ , and  $\{C_{12}E_4\}$ . In addition, for each carbon atom, the dispersion of chemical shift values (i.e., the chemical shift interval that comprises all the

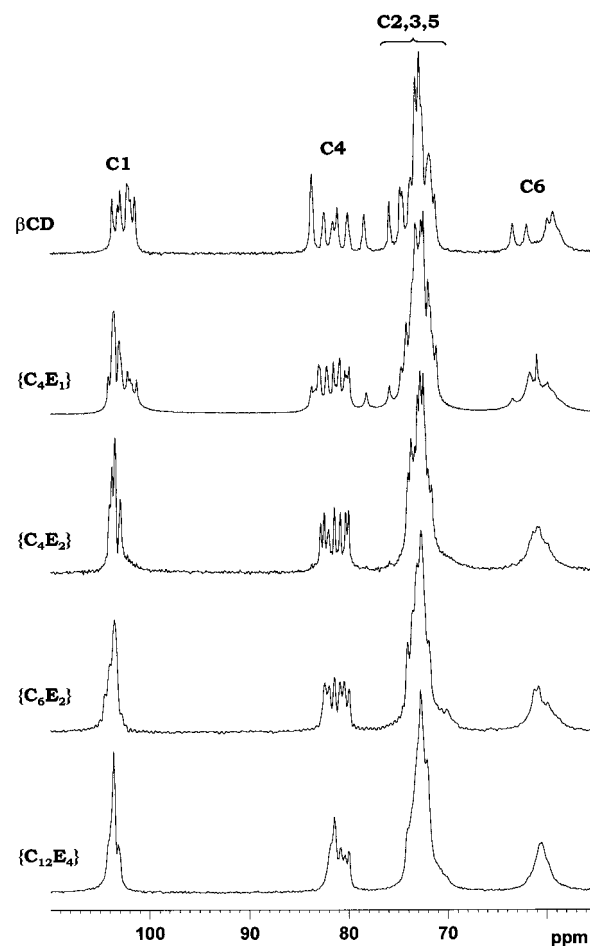


**Figure 6.**  $^{13}\text{C}$  CP MAS NMR spectra for  $\beta$ CD,  $\{C_4E_1\}$ ,  $\{C_4E_2\}$ ,  $\{C_6E_2\}$ , and  $\{C_{12}E_4\}$ , in the  $\beta$ CD region.

**TABLE 1: Amount of Water per  $\beta$ CD Molecule and Dispersion of Chemical Shift Values (ppm) for  $\beta$ CD Carbon Atoms<sup>a</sup>**

system	$n(\text{H}_2\text{O})/\beta\text{CD}$	C1	C4	C2,3,5	C6
$\beta$ CD	10.3	4.2	7.0	6.2	7.0
$\{C_4E_1\}$	11.3	4.6	7.4	6.9	6.8
$\{C_4E_2\}$	10.1–10.7	3.8	5.2	7.2	5.0
$\{C_6E_2\}$	10.2–11.0	3.3	4.2	6.7	5.0
$\{C_{12}E_4\}$	9.0	3.2	3.8	6.5	4.6

<sup>a</sup> Dispersion of the presented values is estimated at  $\pm 0.2$  ppm.

resonances from the same carbon atom) is similar for  $\beta$ CD and  $\{C_4E_1\}$  but decrease monotonically for the remaining inclusion compounds (Table 1). These findings point to an appreciable symmetrization of the  $\beta$ CD macrocycle. Interestingly, the overall shape and dispersion of chemical shift values for the C6 signal seem to reflect the variation in the number of oxyethylene monomers. In fact,  $\{C_4E_2\}$  and  $\{C_6E_2\}$ , whose guests have the same number of oxyethylene units (2), present similar C6 signals, in accord with the previously observed C6 sensitivity to hydrogen bonding of interactions.<sup>8</sup>

It has been previously shown for cyclodextrin inclusion complexes in the solid state that the guest molecules undergo anisotropic motion and that the motion of the smaller guests is least affected by the cavity size of the host.<sup>10</sup> In fact, model calculations carried out for all the herein considered inclusion complexes indicate that  $C_4E_1$  is aligned with the cyclodextrin axis in the lowest energy configuration and has considerable freedom inside the  $\beta$ CD cavity for rotation around its alkyl chain axis.<sup>15</sup> This result agrees with the similarity of the



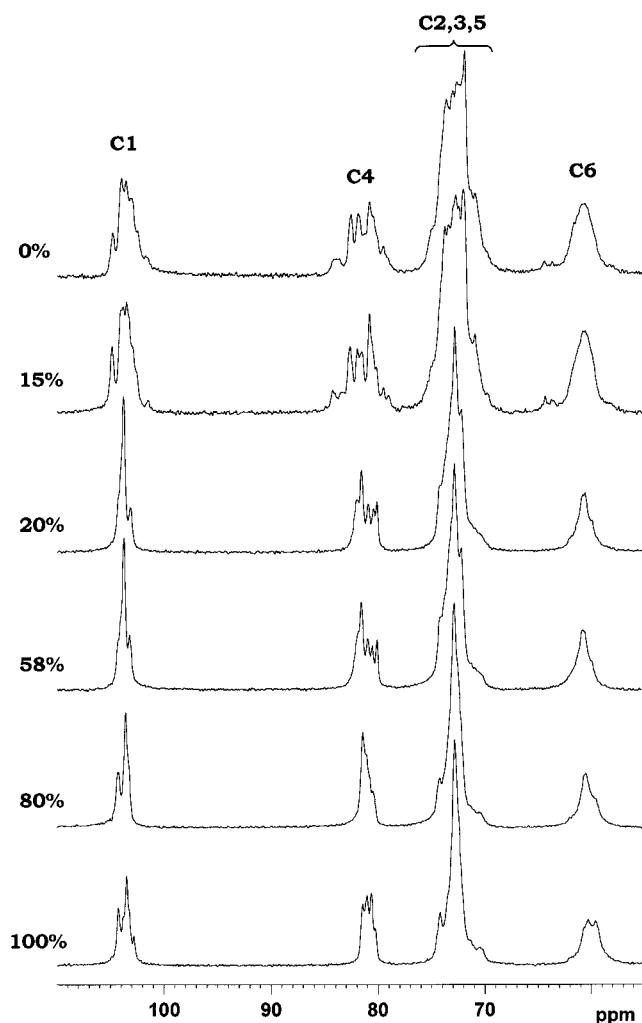


**Figure 7.**  $^{13}\text{C}$  CP MAS NMR spectra for  $\{\text{C}_{12}\text{E}_4\}$  at defined relative humidities, in the  $\beta$ CD region.

dispersions of chemical shift values found for all cyclodextrin carbon atoms in  $\beta$ CD and  $\{\text{C}_4\text{E}_1\}$  (Table 1). The guests of the remaining inclusion compounds ( $\text{C}_4\text{E}_2$ ,  $\text{C}_6\text{E}_2$ ,  $\text{C}_{12}\text{E}_4$ ) interact progressively with the  $\beta$ CD macrocycle through H $\cdots$ H intermolecular contact interactions, because the alkylic chains of these guests become increasingly more flexible. The strongest of these interactions is observed for  $\text{C}_{12}\text{E}_4$  and should reflect the relative length and conformational flexibility of the  $\text{C}_{12}\text{E}_4$  alkylic chain. However, as mentioned above, the multiplicity of all carbon atom signals and the dispersions of chemical shift values observed for  $\{\text{C}_4\text{E}_2\}$ ,  $\{\text{C}_6\text{E}_2\}$ , and  $\{\text{C}_{12}\text{E}_4\}$  are progressively reduced along this series of inclusion compounds. This experimental finding points to the existence of a rotational motion for each of these guests around the  $\beta$ CD axis, to average out the magnetic anisotropy of their tilted alkylic chains. This averaging motional mechanism should be progressively efficient [i.e., the corresponding geometrical factor  $(3 \cos^2 \theta - 1)/2$  should be smaller] along the above-mentioned series of inclusion compounds in order to result in a progressively reduced dispersion of chemical shift values.

Figure 7 shows the  $^{13}\text{C}$  CP/MAS NMR spectra for  $\{\text{C}_{12}\text{E}_4\}$  at defined relative humidities, and Table 2 presents the amount of water per  $\beta$ CD molecule and the dispersions of chemical shift values for  $\beta$ CD carbon atoms in  $\{\text{C}_{12}\text{E}_4\}$ , at defined relative humidities (RHs). The first general observation is that the hydration level appreciably affects the spectra, in particular, the multiplicity of resonances and the dispersion of chemical shifts

**TABLE 2: Amount of Water per  $\beta$ CD Molecule and Dispersion of Chemical Shift Values (ppm) for  $\beta$ CD Carbon Atoms in  $\{\text{C}_{12}\text{E}_4\}$ , at Defined Relative Humidities (RHs)<sup>a</sup>**

RH (%)	$n(\text{H}_2\text{O})/\beta\text{CD}$	C1	C4	C2,3,5	C6
0	8.2	5.4	6.5	8.4	7.3
15	8.3	4.9	6.5	8.4	7.8
20	9.0	3.2	3.8	6.5	4.9
58	9.0	3.4	3.6	6.4	4.5
80	9.0	3.2	2.8	6.1	4.7
100	11.0	3.2	2.7	5.9	4.9

<sup>a</sup> Dispersion of the presented values is estimated at  $\pm 0.2$  ppm.

for each  $\beta$ CD carbon atom. In general terms, two groups of spectra stand out from this figure and table, one formed by humidities 0% and 15%, which present larger dispersions of chemical shift values, the other grouping the remaining humidities. Fully hydrated  $\{\text{C}_{12}\text{E}_4\}$  presents the smallest ranges of chemical shifts, thus showing that hydration water seems to contribute in a relevant way to the symmetrization of the  $\beta$ CD macrocycle.

#### 4. Conclusions

The solid-state inclusion of the nonionic surfactant  $\text{C}_{12}\text{E}_4$  in  $\beta$ CD,  $\{\text{C}_{12}\text{E}_4\}$ , exhibits interesting structural features both as a true inclusion compound and as a crystalline hydrate. Comparison with inclusion compounds of other  $\text{C}_n\text{E}_m$  homologues, like  $\{\text{C}_4\text{E}_1\}$ ,  $\{\text{C}_4\text{E}_2\}$ , and  $\{\text{C}_6\text{E}_2\}$ , reveals peculiar properties for  $\{\text{C}_{12}\text{E}_4\}$ . First of all, thermal dehydration of  $\{\text{C}_{12}\text{E}_4\}$  occurs in a stepwise manner with the largest number of inflection points among these inclusion compounds, suggesting the presence of energetically distinct types of water molecules. The dispersions of  $^{13}\text{C}$  chemical shift values for the C1 and C4 atoms of the  $\beta$ CD macrocycle reveals a progressive reduction along the series  $\{\text{C}_4\text{E}_1\}$ ,  $\{\text{C}_4\text{E}_2\}$ ,  $\{\text{C}_6\text{E}_2\}$ , and  $\{\text{C}_{12}\text{E}_4\}$ , with the latter inclusion compound showing the smallest dispersions. While the same general trend is observed for C6 atoms,  $\{\text{C}_4\text{E}_2\}$  and  $\{\text{C}_6\text{E}_2\}$ , whose guests have the same number of oxyethylene monomers, show the same dispersion, a fact that probably stresses the well-known sensitivity of C6 atoms to hydrogen bonding type of interactions.

As a function of relative humidity, the integrated intensity of the O—H Raman stretching band ( $I_{\text{OH}}$ ) for  $\{\text{C}_{12}\text{E}_4\}$  increases over the whole range of humidities but is approximately constant for humidities between 20% and 80%. This behavior seems to be consistent with the occurrence of energetically distinct hydration water molecules, as revealed by thermogravimetry, and contrasts with  $\beta$ CD, which shows a linear increase of  $I_{\text{OH}}$  from 15% up to 100% of relative humidity and a continuous thermal dehydration.<sup>16,17</sup>

Raman bands in the 895–970  $\text{cm}^{-1}$  region, recorded at defined humidities over the whole range of humidities, reveal an apparent discontinuity in passing from 15% to 20% of humidity, in particular, with the sudden intensity increase of a Raman band at 926  $\text{cm}^{-1}$ . Incidentally, a  $\beta$ CD Raman band at around 920  $\text{cm}^{-1}$  had been previously used as a Raman optical activity signature for the dispersion of conformations around the glycosidic linkage in the  $\beta$ CD macrocycle.<sup>13</sup> Interestingly, the dispersions of the  $^{13}\text{C}$  chemical shift values recorded for  $\{\text{C}_{12}\text{E}_4\}$  at defined humidities also exhibit a discontinuous behavior in passing from 15% to 20% of humidity. These two pieces of experimental evidence seem to suggest the existence of a distinct phase for  $\{\text{C}_{12}\text{E}_4\}$  below 20% of humidity. Incidentally, at low humidities (below 15%), a distinct phase with unknown structure had also been reported for  $\beta$ CD.<sup>3</sup>

Overall, the above findings converge to stress the structural relevance of hydration water in  $\{C_{12}E_4\}$ .

**Acknowledgment.** We are grateful to Prof. João Rocha, for helpful discussions, and to Ms. Claudia Morais, for assistance in the NMR experiments.

## References and Notes

- (1) Steiner, Th.; Koellner, G. *J. Am. Chem. Soc.* **1994**, *116*, 5122.
- (2) Steiner, Th.; Moreira da Silva, A. M.; Teixeira-Dias, J. J. C.; Muller J.; Saenger W. *Angew. Chem., Int. Ed. Engl.* **1995**, *34*, 1452.
- (3) Marini, A.; Berbenni, V.; Bruni, G.; Massarotti, V.; Mustarelli, P.; Villa, M. *J. Chem. Phys.* **1995**, *103*, 7532.
- (4) Lindner, K.; Saenger, W. *Carbohydr. Res.* **1982**, *99*, 103.
- (5) Betzel, Ch.; Saenger, W.; Hingerty, B. E.; Brown, J. M. *J. Am. Chem. Soc.* **1984**, *106*, 7545.
- (6) (a) Usha, M. G.; Witterbort, R. J. *J. Mol. Biol.* **1989**, *208*, 669. (b) Usha, M. G.; Witterbort, R. J. *J. Am. Chem. Soc.* **1992**, *114*, 1541.
- (7) Gidley M. J.; Bociek, S. M. *J. Am. Chem. Soc.* **1988**, *110*, 3820.
- (8) Heyes, S. J.; Clayden, N. J.; Dobson, C. M. *Carbohydr. Res.* **1992**, *233*, 1.
- (9) Saenger, W. *Angew. Chem., Int. Ed. Engl.* **1980**, *19*, 344.
- (10) Hall, L. D.; Lim, T. K. *J. Am. Chem. Soc.* **1986**, *108*, 2503.
- (11) Schick, M. J. (Ed.) *Nonionic Surfactants*, Surfactant Science Series, vol. 23; Marcel Dekker: New York, 1987.
- (12) Turro, N. J.; Kuo, P. C. *Langmuir* **1985**, *1*, 170.
- (13) Bell, A. F.; Hecht, L.; Barron, L. D. *Chem. Eur. J.* **1997**, *3*, 1292.
- (14) Weast, R. C., Ed. *Handbook of Chemistry and Physics*; CRC Press: Cleveland, OH, 1976; p E-46.
- (15) Cunha-Silva, L.; Teixeira-Dias, J. J. C. Unpublished work.
- (16) Nakai, Y.; Yamamoto, K.; Terada, K.; Kajiyama, A.; Sasaki, I. *Chem. Pharm. Bull.* **1986**, *34*, 2178.
- (17) Claudy, P.; Germani, P.; Letoffe, J. M. *Thermochim. Acta* **1990**, *161*, 75.
- (18) (a) Kalyanasundaram, K.; Thomas, J. K. *J. Phys. Chem.* **1976**, *80*, 1462. (b) Cooney, R. P.; Barraclough, C. G.; Healy, T. W. *J. Phys. Chem.* **1983**, *87*, 1868.
- (19) (a) Matsuura, H.; Fukuhara, K. *J. Phys. Chem.* **1986**, *90*, 3057. (b) Matsuura, H.; Fukuhara, K. *J. Polym. Sci. B* **1986**, *24*, 1383. (c) Matsuura, H.; Fukuhara, K. *J. Phys. Chem.* **1987**, *91*, 6139.
- (20) Moreira da Silva, A. M.; Steiner, Th.; Saenger, W.; Empis J.; Teixeira-Dias, J. J. C. *J. Chem. Soc. Chem. Commun.* **1996**, 1871.